Characterization of cold-formed steel shear wall behavior under cyclic loading for the CFS-NEES building

P. Liu[1], K.D. Peterman[2], C. Yu[3], B.W. Schafer[4]

The objective of this paper is to provide a full hysteretic characterization of OSB sheathed cold-formed steel (CFS) shear walls designed for use in the National Science Foundation funded Network for Earthquake Engineering Simulation (NEES) project: CFS-NEES (www.ce.jhu.edu/cfsnees). The shear walls were designed for a two-story ledger-framed building (i.e., the CFS-NEES building) that will undergo full-scale shake table testing at the University of Buffalo NEES site. Shear walls in real construction, such as the CFS-NEES building, have details that differ from the shear walls tested and provided for strength prediction in standards such as AISI-S213-07. Differences include: (a) ledger (rim track) members are attached across the interior face of the studs, (b) OSB panel seams, both horizontal and vertical, may not be aligned with the chord studs or only blocked with strap, (c) interior gypsum board is in place, (d) field studs may have a different thickness or grade from the chord studs, and other differences. In this work, these four highlighted differences (a-d) are specifically explored in a series of shear walls tests loaded via cyclic (CUREE) protocols to determine their hysteretic performance. The test results are compared with AISI-S213-07 and hysteretic material characterizations utilizing an elastic-plastic model (EEEP) and a model capable of exhibiting pinching in the hysteretic loops (Pinching4). Recommendations are made with respect to modeling the shear walls.

[1] Graduate Research Assistant, Department of Resource and Civil Engineering, Northeastern University, China, and Visiting Research Scholar, Department of Civil Engineering, Johns Hopkins University, Baltimore, MD, <pliu23@jhu.edu>

[2] Graduate Research Assistant, Department of Civil Engineering, Johns Hopkins University, Baltimore, MD, <kpeterm1@jhu.edu>

[3] Associate Professor, Department of Engineering Technology, University of North Texas, Denton, TX, <cyu@unt.edu>

[4] Professor and Chair, Department of Civil Engineering, Johns Hopkins University, Baltimore, MD, <schafer@jhu.edu>

1. Introduction

Cold-formed steel has been widely used as a construction material for low and mid-rise buildings due to its light weight and low cost. Common lateral force resisting systems for cold-formed steel construction consist of specifically detailed sheathed and strap braced walls, and other systems (AISI-S213-07). In an effort to develop performance-based seismic design of cold-formed steel systems the CFS-NEES project has recently detailed a two-story archetype building (Madsen et al. 2011). The shear walls in the building utilize back-to-back chord studs, and OSB sheathing. The details of the shear walls deviate modestly from tested configurations in AISI-S213-07 in that (a) a ledger or rim track is attached to the interior face of the walls, (b) gypsum board is attached to the interior face of the walls, (c) OSB panel seams do not always fall at stud or track locations and thus strapping must be used for shear transfer in the walls, and (d) the field studs do not always match the grade or thickness of the chord studs. Given these variations, and a need to have a full hysteretic characterization of the shear walls for model predictions, as well as a general desire to better understand actual building performance for the CFS-NEES building, it was decided to complete a shear wall test series that specifically investigated the impact of these variations on hysteretic performance.

Cold-formed steel shear walls have seen significant study. Notably, based on the work of Serrete (1996, 1997, 2002) the North American Standard for Cold-Formed Steel Framing: Lateral Design (AISI S213-07) provides nominal strength for three different types of sheathing: 15/32 in. “Structural 1” sheathing, 7/16 in. Oriented Strand Board (OSB), and 0.018-0.027 in. steel sheet. Tabled values are based on maximum aspect ratio, fastener spacing at the panel edge, and stud and track thickness. More recently, Rogers (Branston 2004; Branston et al. 2004; Branston, Chen 2004; Chen et al. 2004; Boudreault 2005) has developed a large multi-year shear wall testing program. Among the many aspects studied is the significance of the cyclic loading protocol including comparisons between Sequential Phased Displacement (SPD) and the Consortium of Universities for Research in Earthquake Engineering (CUREE) protocol. In general, the dominant failure modes involved the sheathing-to-steel connection and a combination of fastener pull-through, tear-out, and bearing. A large variety of different sheathing materials and details have been explored, see Cobeen (2010) for a summary. However, the impact of ledger track, panel seams, and grade and thickness of the field studs has not been studied. The test program presented herein is an attempt to broaden the field to include practical details consistent with multi-story CFS buildings.

2. Test program

The complete test program is detailed in the CFS-NEES research report RR03 (Liu et al. 2012) a summary of the testing is provided here.

2.1 Test setup

Monotonic and cyclic shear wall tests were conducted on a 16 ft × 12 ft adaptable testing frame at the University of North Texas. Figure 1 depicts a drawing of the test frame with a 4 ft × 9 ft shear wall specimen.

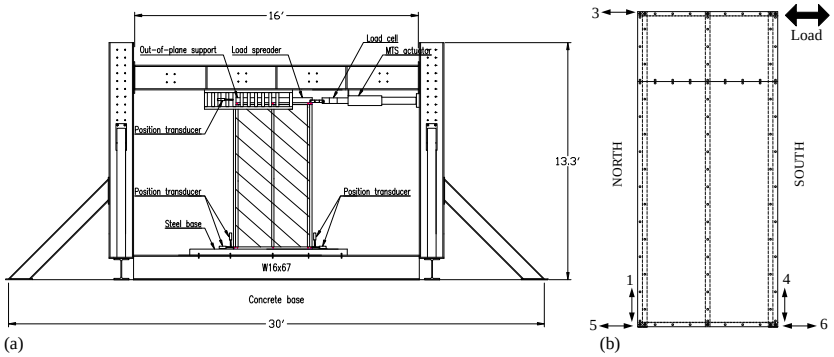

Figure 1 Schematics of (a) testing rig with specimen, and (b) sensor plan on specimen, arrows and numbers correspond to position transducer locations.

Specimens are bolted to the test frame via the steel base, according to the plan detailed in Figure 2. Both hold downs and anchor bolts restricted the specimen from lateral displacement at the bottom of the test frame. At the top of the specimen, a WT shape acts as a load spreader, transferring horizontal force from the hydraulic actuator to the specimen. To ensure effective load transfer, the WT section is attached to the shear wall top track with No. 10 x 1” hex washer head self-drilling screws along two lines, spaced every 3 inches. To keep the shear wall in plane during the test, a series of steel rollers (labeled ‘out-of-plane support’ in Figure 1) are arranged to restrict the motion of the load spreader.

The test frame is equipped with a 35 kip hydraulic actuator with ±5 in. stroke. A 20 kip load cell is pinned to the specimen and actuator. Five position transducers are employed to measure deflection of the shear wall in the north, south, and lateral directions (Figure 1b). Each chord stud is outfitted with vertically- and horizontally-oriented position transducers to capture the tension and compression experienced by the wall. A position transducer at the top of the wall records specimen lateral displacement.

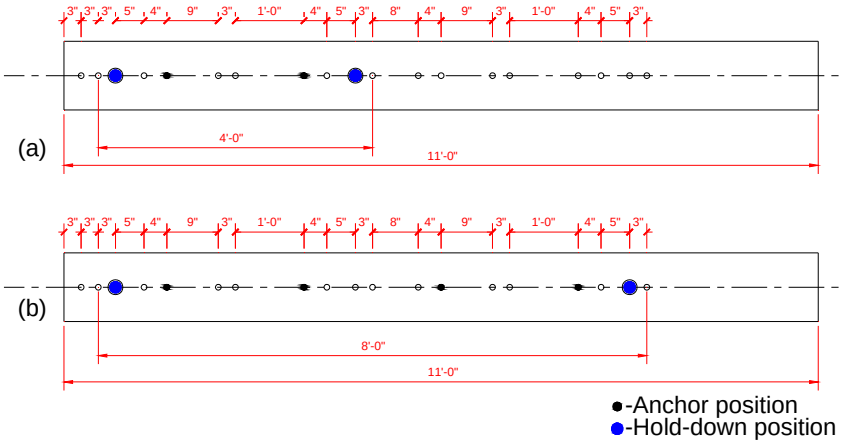

Figure 2 Anchor placement along test frame base (top view) for (a) 4 ft wide walls and (b) 8 ft wide walls.

2.2 Test method

Both monotonic and cyclic tests are performed under displacement control. Monotonic tests follow ASTM E564-06, "Standard Practice for Static Load Test for Shear Resistance of Framed Walls for Buildings." This protocol requires a preload of approximately 10% of the estimated ultimate load to be applied and held for five minutes to seat all connections. This preload is then removed and the specimen is loaded to one-third of the estimated ultimate load. Again, the specimen is loaded and unloaded, this time to two-thirds of ultimate load. The loading continues in this manner until ultimate load is attained.

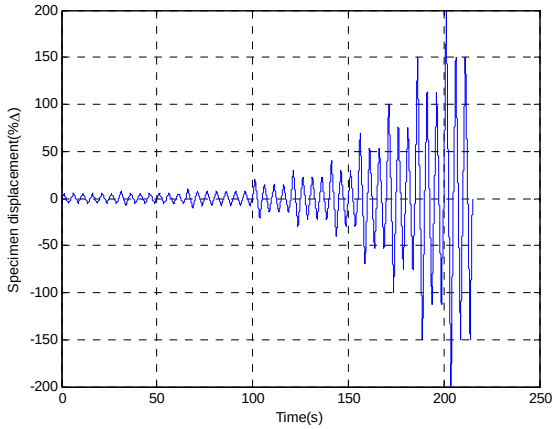

Figure 3 CUREE protocol with cyclic frequency of 0.2 Hz.

For cyclic loading, the CUREE protocol was employed in accordance with ASTM E2126, "Standard Test Methods for Cyclic (Reversed) Load Test for Shear Resistance of Vertical Elements of the Lateral Force Resisting Systems for Buildings." A constant cyclic frequency of 0.2 Hz was chosen for the cyclic test as well as a reference displacement based on the results from monotonic tests. Figure 3 depicts the CUREE protocol used for this test series.

2.3 Specimen

The baseline specimen consisted of either 4 ft × 9 ft or 8 ft × 9 ft walls framed with 600S162-54 (50ksi) studs spaced 24 in. o.c. and connected with No. 10 flathead screws to 600T150-54 (50ksi) track (member nomenclature per AISI-S200-07). Studs were spaced at 24 in. o.c. and braced with CRC as detailed in Figure 4a. Chord studs consisted of back-to-back studs assembled with pairs of No. 10 flathead screws spaced every 12 inches. Simpson Strong-Tie S/HDU6 hold downs were attached on the inward face at the bottom of the chord studs. Twelve No. 14 fasteners attached the hold downs to the chord studs.

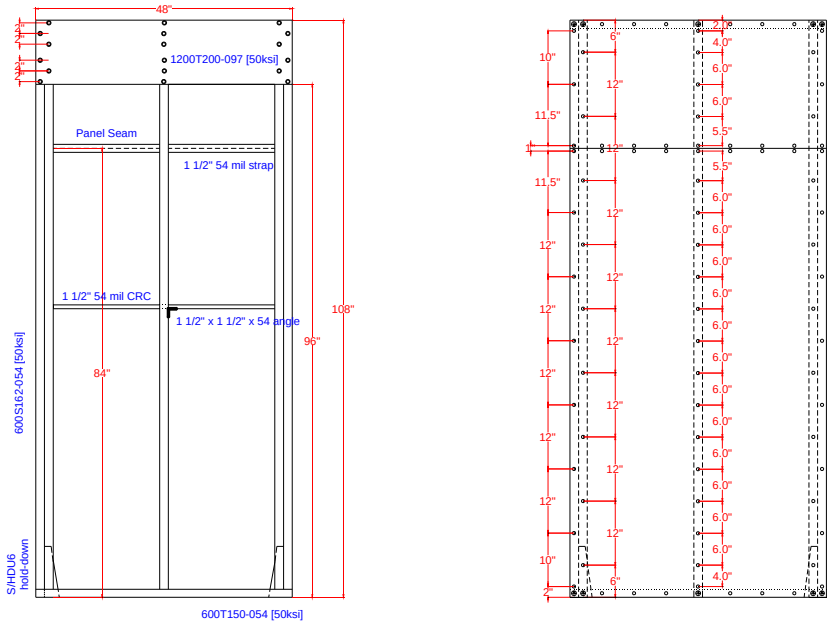

Figure 4: Shear wall specimen drawing (details are the same for 8 ft wide shear walls) (a) back (interior) view, (b) front (exterior) view.

In most cases (see Table 1) 7/16 in. OSB was attached with No. 8 flat head fasteners (1-15/16 in. long) at 6 in. o.c. to the stud and track. When horizontal seams of the OSB do not fall on a track, taught 1 ½ in. wide 54 mil strap was used as shown in Figure 4a. When the rim track/ledger is present (again see Table 1) a 1200T200-097 (50ksi) track is attached with No. 10 fasteners to the top 12 in. of the interior face of the wall. When gypsum board is present 5/8 in. gypsum board is attached with No. 6 fasteners at 6 in. o.c. to the lower 8 ft. (below the 1200T200-097 ledger).

As previously discussed, connection of the shear wall to the testing rig is accomplished in the top track by dragging in the applied shear through two lines of No. 10 fasteners spaced 3 in. o.c. (load spreader of Figure 1a). The bottom track is connected to the steel base (Figure 1a) by 5/8 in. diameter A325 bolts at the hold down locations and directly through the track every 2 ft. along the wall (as detailed in Figure 2(a)).

2.4 Test matrix

The CFS-NEES building dictated specimen construction and design. Most construction variables were studied, including the effect of the ledger (rim track), interior gypsum sheathing (B. Sheathing in Table 1), and panel seam location. Stiffness, strength, and ductility were investigated. The experimental test matrix with selected results is produced in Table 1. It is worth noting that for specimens with a vertical seam not located along a field stud, an additional field stud is added at the seam location. In addition, test 15 employed 33 mil studs in the field (chord studs remained back-to-back 600S162-54 (50ksi)).

Table 1 Test matrix

Test	Load Type	Front Sheathing	Back Sheathing	Stud	Ledger	Horizontal Seam	Vertical Seam	Peak Load	Peak Disp.
quantity	*mono/cyclic*	*OSB*	*Gypsum*	*600S162-xx*	*1200T200-97*	-	-	P_{ave}	Δ_{ave}
unit	–	✔/-	✔/-	1/1000 in.	✔/-	ft	ft	plf	in
1c	Monotonic	✔	–	54	✔	8'up	-	1225	2.96
2	Cyclic	✔	–	54	✔	8'up	-	1102	2.82
3	Cyclic	✔	✔	54	✔	8'up	-	1111	2.67
4	Cyclic	✔	–	54	–	8'up	-	1005	2.40
5	Cyclic	✔	–	54	✔	7'up	-	987	2.39
6	Cyclic	✔	–	54	–	7'up	-	1031	2.24
7	Cyclic	✔	–	54	–	8'up	1'over	897	2.23
8	Cyclic	✔	–	54	–	8'up	2'over	982	3.33
9	Cyclic	✔	–	54	–	8'up	2'over	906	3.56
10	Cyclic	✔	–	54	–	4.5'up	2'over	950	2.95
11c	Monotonic	✔	–	54	✔	8'up	-	1089	2.42
12	Cyclic	✔	–	54	✔	8'up	-	1156	1.96
13	Cyclic	✔	✔	54	✔	8'up	-	1232	1.91
14	Cyclic	✔	–	54	–	8'up	-	1023	1.94
15	Cyclic	✔	–	**33**	–	8'up	-	861	1.64
16	Cyclic	–	✔	54	✔	8'up	-	633	1.47

Note:CUREE protocol employed for cyclic test. *additional field stud 1'over from side. 11r has same configuration as 11c.

3. Test Results

Typical shear-deformation response in the cyclic tests is provided in Figure 5. The limit states in the tested shear walls, specifically fastener pull-through, edge tear out, and fastener bearing are captured in Figure 6. The response is severely pinched as a result of the fastener pull-through mechanism that dominates the nonlinear response.

Maximum strength is observed in the case where the ledger and interior gypsum board are in place (Test 3, Figure 5b), but the best energy absorption (fullest hysteretic loops) appear to occur in the baseline case without the ledger track or interior gypsum board (Test 4, Figure 5c). Key experimental results are provided for all of the conducted tests in Table 2 and full results are provided in the companion CFS-NEES report (Liu et al. 2012).

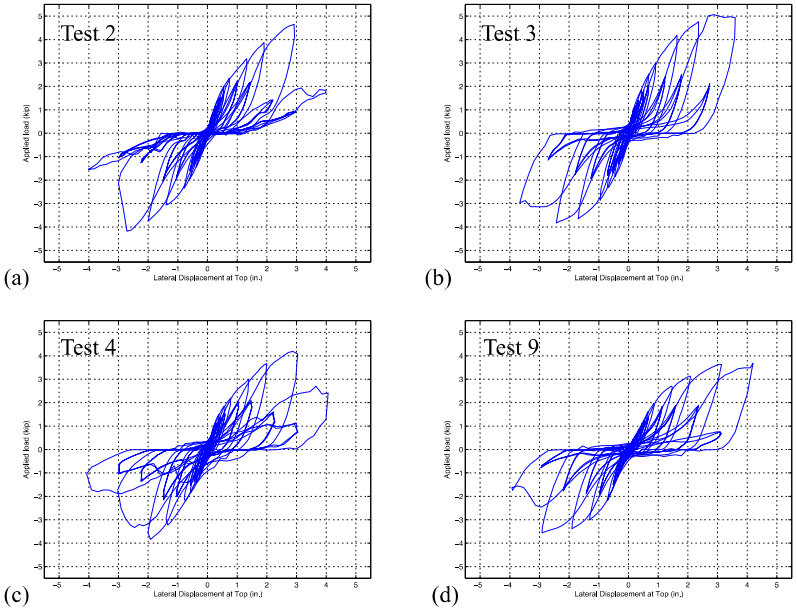

Figure 5 Hysteretic response of 4 ft × 9 ft OSB sheathed shear walls (a) with ledger, (b) and gypsum board, (c) baseline, and (d) extra vertical seam

Figure 6 Detailed shear wall response (a) back of test 4, demonstrating fastener pull-through (PT) along the horizontal seam, (b) front of test 2 depicting the resulting separation of sheathing from seam as a result of PT, (c) separation of OSB from bottom of wall track in test 13, (d) Fastener PT and tear-out (TO) against sheathing along field stud in test 11, and (e) north chord stud in test 13, demonstrating fastener PT in the OSB and a combination of PT and bearing (B) in the gypsum.

Table 2 Summary of test results and hysteretic characterization

Test	Ledger	Gypsum Board	Panel seam varied	33 mil field stud	Basic Test Results			AISI S213 Results[2,6]		EEEP Characterization[3]			Pinching4 Characterization (reloading, unloading ratios) [4]			
					V_{peak}	$\Delta(V_{peak})$	LS[1]	V_n	$\delta(V_{peak})$	$\Delta(0.4V_{peak})$	Δ_{max}	V_y	r_{+D}	r_{+V}	u_{+V}	r_{-V}
					plf	in.		plf	in.	in.	in.	plf	-	-	-	-
1c	✔	-	-	-	1225	2.96	PT	836	2.96	0.61	3.31	1078	-	-		-
2	✔	-	-	-	1102	2.82	PT	836	2.46	0.49	3.06	904	0.60	0.10	-0.08	0.20
3	✔	✔	-	-	1111	2.67	PT	836	2.50	0.42	3.26	962	0.31	0.15	-0.08	0.25
4	-	-	-	-	1005	2.40	PT	836	2.10	0.45	2.81	838	0.50	0.32	-0.08	0.35
5	✔	-	✔	-	987	2.39	PT	836	2.04	0.47	2.78	841	0.60	0.11	-0.08	0.11
6	-	-	✔	-	1031	2.24	PT	836	2.20	0.49	2.50	857	0.30	0.15	-0.08	0.35
7	-	-	✔	-	897	2.23	PT	836	1.73	0.45	3.30	792	0.38	0.15	-0.08	0.12
8	-	-	✔	-	982	3.33	PT	836	2.02	0.44	3.65	852	0.30	0.15	-0.08	0.18
9	-	-	✔	-	906	3.56	PT	836	1.76	0.53	3.51	818	0.35	0.10	-0.08	0.30
10	-	-	✔	-	950	2.95	PT	836	1.91	0.51	3.70	821	0.28	0.16	-0.08	0.16
11c	✔	-	-	-	1089	2.42	PT+B	940	1.61	0.36	2.91	957	-	-		-
12	✔	-	-	-	1156	1.96	PT+B	940	1.79	0.34	2.22	1007	0.14	0.16	-0.08	0.18
13	✔	✔	-	-	1232	1.91	PT+B	940	2.01	0.33	2.14	1076	0.28	0.16	-0.08	0.16
14	-	-	-	-	1023	1.94	PT+B	940	1.44	0.25	2.14	906	0.50	0.18	-0.08	0.15
15	-	-	-	✔	861	1.64	PT	700	1.58	0.29	2.11	743	0.50	0.16	-0.08	0.18
16	✔	✔	-	-	231	1.47	PT	-	-	0.09	3.31	213	0.60	0.10	-0.08	0.16

Pinching4 Characterization[5] - Envelope Backbone Curve

	$^{+}V_1$	$^{+}V_2$	$^{+}V_3$	$^{+}V_4$	$^{+}\Delta_1$	$^{+}\Delta_2$	$^{+}\Delta_3$	$^{+}\Delta_4$	$^{-}V_1$	$^{-}V_2$	$^{-}V_3$	$^{-}V_4$	$^{-}\Delta_1$	$^{-}\Delta_2$	$^{-}\Delta_3$	$^{-}\Delta_4$
	plf	plf	plf	plf	in.	in.	in.	in.	plf	plf	plf	plf	in.	in.	in.	in.
2	465	930	1162	468	0.50	1.77	2.92	2.95	-417	-834	-1043	-259	-0.48	-1.65	-2.71	-2.82
3	506	1011	1264	624	0.49	1.56	2.87	3.58	-383	-767	-958	-480	-0.35	-1.15	-2.43	-3.66
4	418	837	1046	523	0.47	1.70	2.88	4.06	-385	-771	-963	-482	-0.42	-1.25	-1.92	-4.08
5	409	819	1023	334	0.56	1.56	2.83	2.99	-380	-760	-950	-591	-0.37	-1.20	-1.96	-2.21
6	458	916	1145	495	0.46	1.32	2.78	3.06	-348	-696	-870	-495	-0.49	-1.35	-1.69	-2.05
7	351	702	878	439	0.51	1.41	2.55	4.08	-366	-733	-916	-458	-0.37	-1.07	-1.91	-4.03
8	415	830	1037	519	0.45	1.65	3.65	4.12	-371	-742	-928	-462	-0.42	-1.30	-3.00	-4.01
9	367	734	917	459	0.61	1.78	4.20	4.20	-358	-715	-894	-443	-0.45	-1.19	-2.92	-3.90
10	381	761	952	476	0.56	1.68	2.91	4.10	-380	-759	-949	-475	-0.45	-1.32	-2.98	-4.06
12	503	1005	1257	448	0.35	1.08	2.27	2.43	-422	-844	-1055	-382	-0.32	-0.90	-1.66	-1.96
13	531	1062	1327	532	0.40	1.10	2.20	2.31	-455	-910	-1137	-640	-0.26	-0.84	-1.62	-1.95
14	423	846	1057	208	0.27	0.90	2.22	2.23	-372	-744	-989	-280	-0.21	-0.61	-1.66	-1.91
15	353	706	883	442	0.31	0.98	1.62	3.57	-336	-671	-839	-441	-0.27	-0.78	-1.67	-3.51
16	101	202	252	126	0.11	0.59	1.22	3.60	-84	-167	-209	-105	-0.07	-0.26	-1.73	-3.52

1. Limit states: PT = fastener pull-through and B = fastener bearing.

2. V_n per AISI-S213-07 Table C2.1-3 includes 2w/h correction on 4 x 9 walls based on 940 plf (54 mil) instead of 825 plf (43 or 54 mil), and δ per Eq. C2.1-1,shear demand is at V_{peak} for δ.

3. Δ_{max} = deflection when post-peak V is $0.8V_{peak}$, V_y balances area under curve (energy).

4. See note 5 for backbone, reloading: $r_{-D}=r_{+D}$, unloading: $u_{-V}=u_{+V}$

5. 4 pt backbone defined by $\Delta_1=\Delta(0.4V_{peak})$, $\Delta_2=\Delta(0.8V_{peak})$, $\Delta_3=\Delta(V_{peak})$, Δ_4 deflection past peak at next larger CUREE cycle if $<0.5Vpost_{peak}$ otherwise max Δ at $0.5V_{postpeak}$

6. Test 15, V_n capacity based on 700 plf due to 33 mil field studs, chords should still be designed for 940 plf based on 54 mil chord studs

4. Hysteretic Characterization of Shear Walls

4.1 Equivalent Energy Elastic-Plastic (EEEP) Model

The simplest and most commonly used model for characterizing the nonlinear response of cold-formed steel framed shear walls is the equivalent energy elastic-plastic (EEEP) model. Area under the envelope backbone curve is equated to an elastic-plastic model. Area up to the post-peak deflection at which the shear strength reaches 80% of its peak shear value is included in the energy balance. Initial elastic stiffness is determined based on the tested response at 40% of the peak shear capacity ($0.40V_{peak}$) and plastic shear capacity (V_y) is set so that the area under the model and tested (envelope) curve is the same. Results are provided in Table 2 and further detailed in Liu et al. (2012).

4.2 Hysteretic model with pinching (Pinching4) Model

A key feature of the tested shear walls that is not captured in the EEEP model is the "pinching" of the hysteretic loops as shown in Figure 5. Therefore, characterization with a more advanced Pinching 4 hysteretic model (Lowes et al 2004) as implemented in OpenSees (McKenna and Rodgers 2011) was pursued. The key features of this model are illustrated in Figure 7. The model allows for a 4-point multi-linear backbone envelope in both positive (+) and negative (-) displacements. Unloading and reloading are handled by a series of force and displacement ratios (r_Δ, r_V, u_V also which may vary in + and -) that operate on the maximum/minimum displacement experienced in the loading history. Additional degradation parameters available in the model were not utilized here.

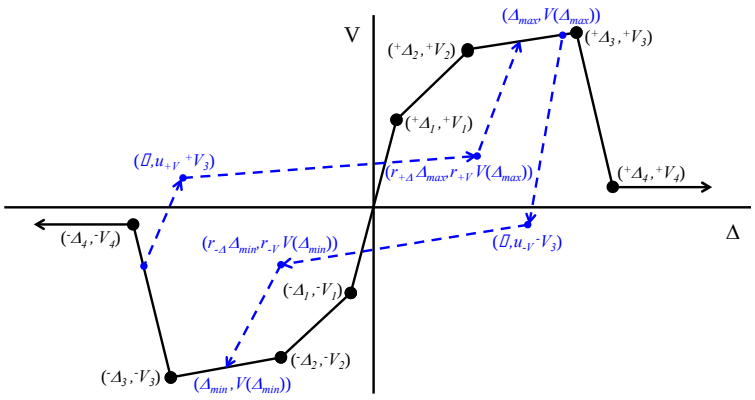

Figure 7 Pinching4 uniaxial material model implemented for a shear wall

A complete set of Pinching4 parameters were fit to the tested shear walls and are reported in Table 2. The envelope backbone curve is defined by selecting points 1 to 3 to coincide with $0.40V_{peak}$, $0.80V_{peak}$, and V_{peak} (for both + and -). The 4th point includes the degradation in post peak strength, it was decided that this degradation must be at least 50% of V_{peak}. Therefore the 4th point is the peak force level for the next cycle in which Δ exceeds the previous Δ_{max} (this occurs every 3rd cycle in the CUREE protocol as shown in Figure 3) if that force level is less than or equal to $0.50V_{peak}$; otherwise the maximum recorded deflection in the test is utilized but the force level is not allowed to be any greater than $0.5V_{peak}$. This reflects the fact that Pinching4 assumes the specimen can deliver the force at the 4th envelope point for all large Δ, as shown in Figure 7.

4.3 Example Comparison of EEEP and Pinching4 Models

The EEEP and Pinching4 models are compared to the results of Test 12 in Figure 8. The Figure shows the complete hysteretic response followed by selected cycles in the CUREE protocol. Cycle 38 of Figure 8 includes the peak shear capacity (V_{peak}) and cycles 39 and 41 are post-peak cycles. Cycle 39 is for a Δ that is 75% of cycle 39 and cycle 41 is for a Δ that is 150% of cycle 39.

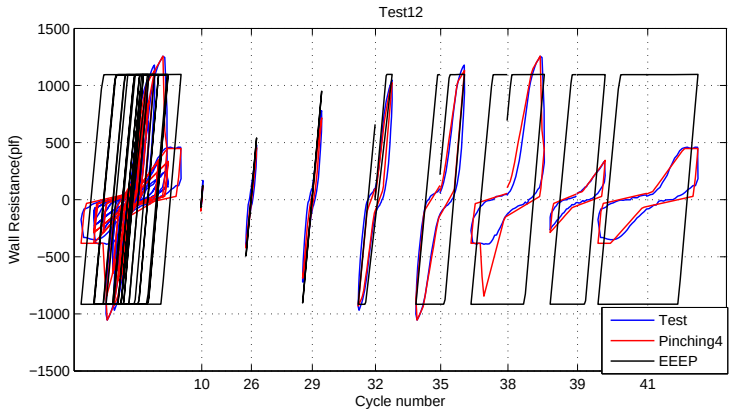

Figure 8 Typical Curve fitting side by side

Figure 8 illustrates that EEEP is only appropriate for uni-directional pushover analysis; the model is completely inappropriate for full cyclic response as it grossly over-predicts the energy dissipation capability since pinching is ignored. Properly calibrated the Pinching4 model provides a fine approximation of the actual shear wall response. However, in individual cycles (see -Δ in cycle 38) errors may still persist. Nonetheless, stiffness and strength as well as total and

per-cycle energy are captured well even when highly degraded (cycles 39, 41, etc.) and the model is recommended for use in nonlinear time history analysis.

5. Discussion

5.1 AISI S213-07 Strength

The nominal shear strength, V_n, as reported in Table 2 per AISI-S213-07 for shear walls with 54 mil studs utilizing 7/16 in. OSB sheathing attached at 6 in. o.c. with No. 8 fasteners on one side, is 940 plf. The 4 ft × 9 ft ($w \times h$) shear walls slightly violate the maximum 2:1 aspect ratio and are corrected via the $2w/h$ factor down to 836 plf. Test 15, which uses 33 mil field studs, may be conservatively estimated with respect to strength based on 33 mil tabled values resulting in a predicted V_n of 700 plf. (Note, the chord studs should still be designed for the maximum possible delivered capacity, i.e. 940 plf).

Tested capacity (V_{peak}) is greater than nominally specified (V_n) values in all tested cases. Tests 3 (4 ft × 9 ft) and 13 (8 ft × 9 ft), which have both the ledger and the gypsum board in place, have the greatest overstrength: 30% greater than V_n. Tests 4 (4 ft × 9 ft) and 14 (8 ft × 9 ft), which are essentially the baseline case, have overstrength of 20% and 10%. Tests where the panel seam is varied have the least overstrength. In fact, Tests 7 and 9 which include additional vertical seams in the 4 ft × 9 ft specimens have tested capacities less than 940 plf, but still greater than the 836 plf that results after the $2w/h$ aspect ratio correction.

Test 15 replaces the 54 mil field studs with 33 mil field studs (this is consistent with the lighter demands on field studs and gravity framing in the upper story of the CFS-NEES building). This too results in a modest reduction in strength below 54 mil specified values. If, conservatively, 33 mil values are selected from AISI-S213-07 then the nominal values is only 700 plf, compared with the tested 861 plf which is well in excess of the nominal. Thus, as long as the designer accounts for the potential reduction due to the field studs strength is not compromised; though "overstrength" in such cases should be explicitly considered as the expected strength is between the 33 mil and 54 mil values.

5.2 AISI S213-07 Deflection

Deflection (δ) per AISI-S213-07 is provided in Table 2. For convenience δ is calculated at V_{peak} instead of at V_n so that it may be compared directly to the tested deflection at peak shear: Δ. In general, test deflections (Δ) are greater than calculated deflections (δ), on average by 27%. Tests 4 (4 ft × 9 ft) and 14 (8 ft × 9 ft), which are the baseline case with no ledger or gypsum board and conventional 4 ft × 8 ft OSB panel sheets employed, have test Δ 14% and 35%

greater, respectively, than AISI-S213-07 δ. Depending on the panel seam location AISI-S213-07 can drastically underestimate deflection; for example, Test 15 has a Δ 202% greater than δ. Predictions for the 8 ft × 9 ft walls are generally better than the 4 ft × 9 ft walls.

5.3 Ledger Track

The use of ledger framing, and thus the presence of a ledger track, is a unique feature of the CFS-NEES building. The shear wall tests do not include a continuous ledger, but rather a short piece of 1200T200-097 track (the same width as the tested wall), as detailed in Figure 4a. The ledger has an appreciable impact on the strength of the wall. When compared with the Test 4 (4 ft × 9 ft) and Test 14 (8 ft × 9 ft) baselines the addition of the ledger increases strength by 10% and 13%, respectively. However, the hysteresis loops are not quite as full (less energy dissipation). In observing the tests the primary visual difference is in the panel deformations in the top 1 ft, i.e., 9 ft high walls with a 1 ft deep ledger in place visually perform as if they are 8 ft high walls.

5.4 Gypsum Board

The use of interior gypsum board was explored in the testing. Specifically, interior 5/8 in. gypsum board was added to specimens that already had an interior ledger track in place. When compared with the Test 4 (4 ft × 9 ft) and Test 14 (8 ft × 9 ft) baselines the addition of the ledger and gypsum board increases strength by 11% and 20%, respectively (as compared to 10% and 13% increases with just the ledger). Thus, the gypsum board has an appreciable impact on the 8 ft × 9 ft, but not the 4 ft × 9 ft tests. The hysteresis loops are not as full for the ledger + gypsum board case as the baseline. Exterior gypsum board layers are not investigated in this research.

5.5 Chord stud and field stud

Test 14 and 15 demonstrate that that the grade and thickness of field studs have an impact on shear strength, ductility, and stiffness. The shear strength of test 14 (54mil steel, 50ksi field studs) is 16% higher than that of test 15 (33mil steel, 33ksi field studs) even though the back-to-back chord studs, track, sheathing, and ledger are identical. Thus, all of the perimeter fasteners are under identical conditions; nonetheless, the contribution from the fasteners in the field is significant enough to reduce the observed strength. As discussed in Section 5.1 it is recommended to use the 33 mil AISI-S213 values for determining the shear wall capacity, but size the chords and collectors for the 54 mil capacity.

5.6 Panel Seams

Since OSB and gypsum board are typically available only in 4 ft × 8 ft panels, multiple panels or parts of panels are necessary to accommodate walls with

other dimensions. As a result, panel seams are common in construction. Panel seams, however, are not considered in AISI-S213-07 as previous tests have been limited to specimens without seams. Figure 4a depicts the standard horizontal seam detail, a taught strap connecting the two panel seams via fasteners (allowing shear force transfer). For vertical seams, an additional field stud is added if the panel seam does not fall along a stud line. Various horizontal and vertical seams (summarized in Table 1) are introduced into standard wall widths to investigate the influence of panel seams.

The following was observed: overall the presence of additional panel seams in a wall has only a modest impact (a few percent) on the initial stiffness and peak strength. The introduction of vertical panel seams, at least with narrow panels, provides the greatest difference from baseline (as seen in tests 8 and 9). Conclusions on horizontal seams are tied to the presence or lack of a ledger: when the ledger and horizontal panel seam are aligned (tests 2 and 4) the strength is greatest with the ledger in place, but when the ledger and panel seams are at different heights (tests 5 and 6) the strength is greater without the ledger. The most beneficial location for the horizontal seam is when it is aligned with the ledger; essentially creating a fully blocked condition at that seam height.

The test results exhibited modest sensitivity to the introduction of panel seams in the shear walls. To explore the origin of this sensitivity an approach that utilizes the performance of isolated panel-fastener-stud connections to build up the complete shear wall response (Folz and Filliatrault, 2002) is explored. The method is popular in the prediction of wood-framed shear walls and is currently implemented in SAPWood (Pei and van de Lindt 2010).

SAPWood-Nail Pattern analysis was completed where the individual “nail” response was based on a bi-linear model fit to isolated lateral stiffness testing of 7/16 in. OSB attached to a 0.054 in. thick stud with #8 fasteners (Peterman and Schafer 2012). The predicted monotonic shear wall response based on the explored fastener/seam configurations is provided in Figure . Horizontal seams, when compared to a hypothetical seamless model (b), show little to no effect on strength or stiffness. Their location along the wall does not have a significant effect. This behavior is confirmed by the peak shear values attained by tests 4 and 6: both achieved 1031 plf in the model. Peak displacements were impacted by the seam location; test 4 displaces 7% more than test 6 at peak load. Ultimately, this is a finite difference, and potentially within testing error.

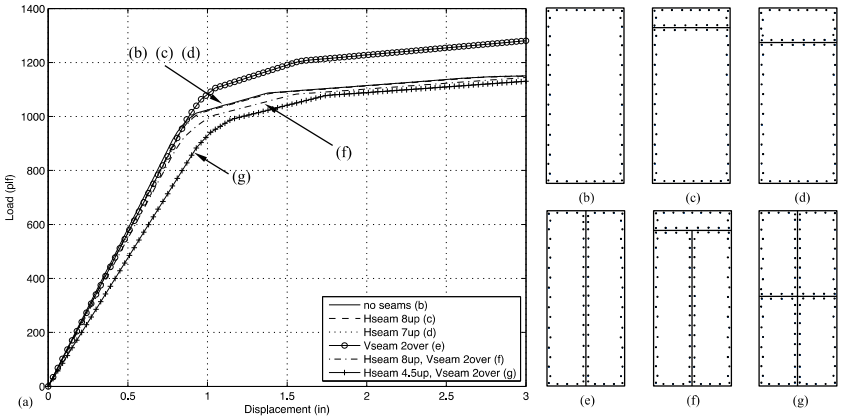

Figure 9 SAPWood-Nail Pattern analysis of 4 ft x 9 ft shear walls: (a) strength and stiffness comparison via bilinear spring approximation for walls with seams and fasteners as shown, for (b) theoretical "no seam" model, (c) test 4, (d) test 6, (e) theoretical vertical seam 2 ft from side, (f) test 9, and (g) test 10.

Out of the four tests modeled herein, test 9 was demonstrated to be the weakest under shear loads (V_{peak} = 906 plf). However, the SAPWood models do not corroborate this relative behavior. Figure 9(a) illustrates that the model corresponding to test 10 is the least stiff and the weakest. Experimentally, test 10 attained a peak shear force of 950 plf (weaker than baseline, but experimentally not the weakest). The SAPWood models do capture that horizontal and vertical seams combined, as in models (f) and (g) are detrimental to strength and stiffness. Additional work utilizing full cyclic tests of the fasteners and comparing the full hysteretic response utilizing the SAPWood-Nail Pattern Analysis models are underway.

7. Conclusions

A series of cyclic (CUREE protocol) tests were conducted on 4 ft × 9 ft and 8 ft × 9 ft OSB sheathed cold-formed steel shear walls. The primary energy dissipation mechanism occurs at the fastener-to-sheathing connection and involves fastener tilting and bearing as well as pull-through, and in some cases edge tear-out. Overall, the hysteretic behavior shows a severely pinched response. Equivalent energy elastic plastic (EEEP) and Pinching4 models are fit to the tested data. It is shown that the EEEP models are only appropriate for static pushover analysis and Pinching 4 models are capable of reasonably

capturing the full hysteretic response including degradation and are recommended for use in nonlinear time history analysis. The shear walls included practical construction details consistent with the recently designed CFS-NEES archetype model building. All tested walls had strength that exceeded specification provided (AISI-S213-07) nominal capacities; however construction details were shown to impact the shear wall behavior. The results indicated that the presence of the ledger track increases shear wall strength (approximately 10%), but modestly decreases energy dissipation. Interior gypsum board increases initial stiffness and may modestly increase strength, but otherwise behaves similar to cases with a ledger track and no interior gypsum. The use of interior field studs with a lower thickness or grade than the chord studs does impact the shear wall strength, and recommendations for determining the shear wall capacity and maximum delivered strength (for design of the chords) is provided. The presence of panel seams in the interior of the shear walls is shown to decrease the strength and increase the flexibility of the shear walls, particularly in the case of vertical panels seams. The results from this study are currently being utilized in modeling of the CFS-NEES building.

Acknowledgments

The donation of materials by ClarkDietrich™ Building Systems and Simpson Strong-Tie Company, Inc. are acknowledged. The shear wall test program was conducted at the University of North Texas. A special thanks to Roger Rovira, Marcus Sanchez, and Noritsugu Yanagi for their help during the shear wall assembling and testing. This report was prepared as part of the U.S. National Science Foundation sponsored CFS-NEES project: NSF-CMMI-1041578: NEESR-CR: Enabling Performance-Based Seismic Design of Multi-Story Cold-Formed Steel Structures. The project also received supplementary support and funding from the American Iron and Steel Institute. Project updates are available at www.ce.jhu.edu/cfsnees. Any opinions, findings, and conclusions or recommendations expressed in this publication are those of the author(s) and do not necessarily reflect the views of the National Science Foundation, nor the American Iron and Steel Institute.

References

AISI-S200-07 (2007). North American Standard for Cold-Formed Steel Framing – General Provisions. American Iron and Steel Institute, Washington, D.C., AISI-S200-07.

AISI-S213-07 (2007). North American Standard for Cold-Formed Steel Framing – Lateral Provisions. American Iron and Steel Institute, Washington, D.C., AISI-S213-07

ASTM E2126 (2011). "Standard Test Methods for Cyclic (Reversed) Load Test for Shear Resistance of Vertical Elements of the Lateral Force Resisting Systems for Buildings," ASTM International, West Conshohocken, PA, 2006, DOI: 10.1520/E2126-11

ASTM E564 (2006). "Standard Practice for Static Load Test for Shear Resistance of Framed Walls for Buildings," ASTM International, West Conshohocken, PA, 2006, DOI: 10.1520/E0564-06

Boudreault, F.A. (2005). Seismic analysis of steel frame / wood panel shear walls. M. Eng. thesis, Department of Civil Engineering and Applied Mechanics, McGill University, Montréal, Quebec.

Branston, A.E. (2004). Development of a design methodology for steel frame / wood panel shear walls. M. Eng. thesis, Department of Civil Engineering and Applied Mechanics, McGill University, Montréal, Quebec

Branston, A.E., Boudreault, F.A., Chen, C.Y., and Rogers, C.A. (2004). Light gauge steel frame / wood panel shear wall test data: summer 2003. Research Report, Department of Civil Engineering and Applied Mechanics, McGill University, Montréal, Quebec.

Chen, C.Y. (2004). Testing and performance of steel frame / wood panel shear walls. M. Eng. thesis, Department of Civil Engineering and Applied Mechanics, McGill University, Montréal, Quebec.

Chen, C.Y., Boudreault, F.A., Branston, A.E., and Rogers, C.A. (2005). "Behaviour of light gauge steel-frame – wood structural panel shear walls". Canadian Journal of Civil Engineering, 33:573–587.

Cobeen, K. (2010). "Cold-Formed Steel Framing Seismic Design Optimization Project, Phase 1a: Seismic Equivalency Parameter Evaluation Research." Wiss, Janney, Elstner Associates, Inc., Report RP10-4, American Iron and Steel Institute, Washington, DC.

Filiatrault, A., and Folz, B., (2002). "Performance-Based Seismic Design of Wood Framed Buildings", ASCE, Journal of Structural Engineering, Vol. 128, No. 1, 39-47.

Liu, P. Peterman, K.D. and Schafer, B.W. (2012). “Shear wall test report for the CFS-NEES Building.” CFS-NEES-RR03, www.ce.jhu.edu/cfsnees.

Lowes, L., Altoontash, A. (2003). “Modeling reinforced-concrete beam-column joints subjected to cyclic loading,” ASCE, Journal of Structural Engineering, 129:12:1686-97.

Madsen, R.L., Nakata, N., Schafer, B.W. (2011). “CFS-NEES Building Structural Design Narrative.” CFS-NEES-RR01, www.ce.jhu.edu/ cfsnees.

McKenna, F., and Rodgers, G. (2011), "OpenSees binary and source code; no GUI," http://nees.org/resources/openseesbuild.

Pei, S.,van de Lindt, J. (2010). “User’s Manual for SAPWood for Windows.” http://nees.org/resources/sapwood.

Peterman, K.D., and Schafer, B.W. (2012). “Fastener test report for the CFS-NEES Building.” CFS-NEES-RR04, www.ce.jhu.edu/cfsnees

Serrette, R.L. (1997). “Additional Shear Wall Values for Light Weight Steel Framing.” Report No. LGSRG-1-97, Santa Clara University. Santa Clara, CA.

Serrette, R.L. (2002) “Performance of Cold-Formed Steel –Framed Shear walls: Alternative Configurations,” Final Report : LGSRG-06-02, Santa Clara University. Santa Clara, CA.

Serrette, R.L., Nguyen, H., Hall, G. (1996). “Shear wall values for light weight steel framing.” Report No. LGSRG-3-96, Santa Clara University. Santa Clara, CA.

Vieira Jr., L. C. M., Schafer, B.W. (2012). “Lateral Stiffness and Strength of Sheathing Braced Cold-Formed Steel Stud Walls.” Elsevier, Engineering Structures. 37, 205–213

Yu, C., Chen, Y. (2009). “Steel Sheet Sheathing Options for Cold-Formed Steel Framed Shear Wall Assemblies Providing Shear Resistance - Phase 2, Research Report.” RP09-2, American Iron and Steel Institute, Washington, D.C..

Yu, C., Huang, Z., Vora, H. (2009).“Cold-Formed Steel Framed Shear Wall Assemblies with Corrugated Sheet Steel Sheathing.” Proceedings of the Annual Stability Conference, Structural Stability Research Council, Phoenix, AZ, April 2009.